Homogenization of the Eddy Current Problem in 2D

K. Hollaus, and J. Schöberl

Institute for Analysis and Scientific Computing, Wiedner Hauptstr. 8, A-1040 Vienna, Austria
E-mail: karl.hollaus@tuwien.ac.at

***Abstract*—Homogenization represents a promising method to simulate eddy current losses in laminated iron cores efficiently. First, multi-scale homogenization is demonstrated by a multi-scale approach in the context of an electrostatic problem. Then, multi-scale homogenization is extended to the eddy current problem. Two multi-scale approaches for the magnetic vector potential have been derived to simulate the eddy current losses of a laminated iron core in 2D efficiently and accurately. A rather coarse finite element grid suffices to approximate the homogenized solution of laminated media accurately. A representative numerical example for the electrostatic problem and one for the eddy current problem are presented to demonstrate the validity of multi-scale homogenization, the accuracy of the homogenized solution and to compare the computational costs.**

***Index Terms*—Eddy current losses, finite element method, lamination, multi-scale homogenization.**

I. Introduction

The simulation of eddy current losses in laminated iron cores by the finite element method modeling each lamination individually is not a feasible way. Many elements have to be used in such a model leading to a large equation system. Homogenization overcomes the problem. An efficient and accurate simulation of these losses is still a challenging task [1]-[9]. In the simplest way, homogenization have been carried out by applying anisotropic material properties in finite element models ([2]-[7]) for laminated cores. Such an analysis yields eddy current losses which are to small because the losses caused by the main magnetic flux parallel to the laminations are neglected. Therefore, the solution obtained by this method is frequently corrected in a second step exploiting different approaches, i.e. [4]-[7]. A homogenization method has been proposed in [8], which enforces a symmetric magnetic flux density distribution across the laminations. The homogenization method developed in [9] elimates the restriction of [8]. Contrary to [4]-[9] the present method is based on multi-scale homogenization and determines a contineous tangential magnetic field intensity across the interface between the laminated core and air in one step and it requires only a matrix-vector and a vector-vector multiplication to calculate the losses.

Simply speaking the multi-scale approaches derived in this work make use of the fact that the solution in a laminated medium can be observed as a superposition of a mean value with a perturbation caused by the laminations. Two approaches to calculate the magnetic vector potential were derived describing the eddy currents in laminated iron cores and capable to treat a laminated core efficiently as a bulk without the necessity to model the laminations individually.

In Section II a general boundary value problem with a laminated medium is defined. For the sake of simplicity, multi-scale homogenization is discussed in III by an electrostatic problem first. The approaches for multi-scale homogenization of the eddy current problem with iron cores are presented in section IV. Only linear material properties are considered. Accuracy and computational costs of multi-scale homogenization are shown by numerical examples.

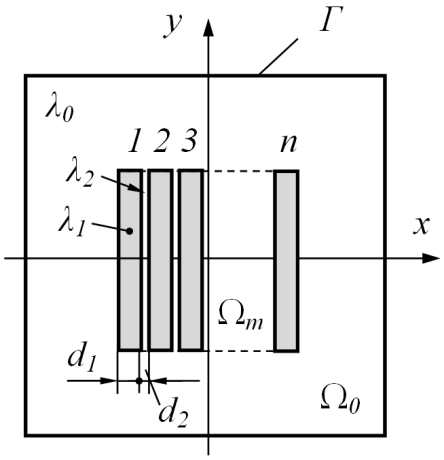

Fig. 1. Boundary value problem with laminated media.

II. Boundary Value Problem with a Laminated Medium

A general boundary value problem is shown in Figure 1. The computational domain Ω consists of a laminated medium Ω_m surrounded, for instance, by air Ω_0:

$$\Omega = \Omega_m \cup \Omega_0 \tag{1}$$

A specific partial differential equation holds in each domain Ω_i and either Dirichlet, Neumann or Robin boundary conditions are given on the boundary of the entire domain Ω,

$$\Gamma = \Gamma_D \cup \Gamma_N \cup \Gamma_R. \tag{2}$$

There are n laminations in Ω_m. The material parameters λ_0, λ_1 and λ_2 are valid in air, in the laminations and in the gap, respectively. Of course several parameters are possible in one domain too. The thickness of a lamination is denoted by d_1 and the width of the gap by d_2. The laminated medium is assumed to be constructed periodically. A fill factor f is defined as

$$f = \frac{d_1}{d_1 + d_2}, \tag{3}$$

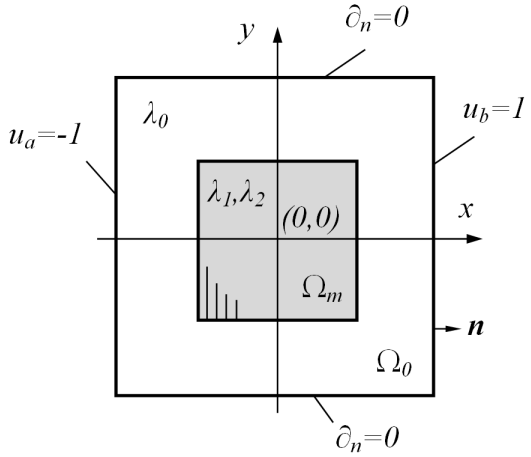

Fig. 2. Boundary value problem: Specific electrostatic problem.

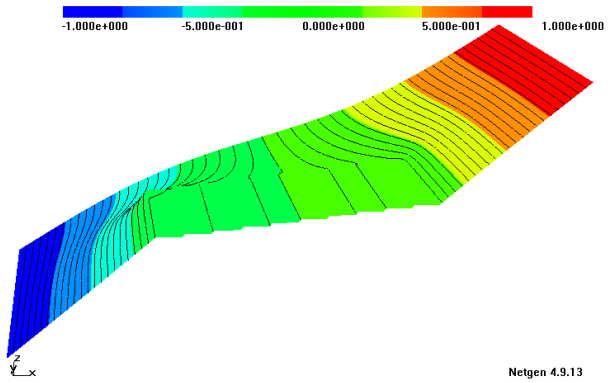

Fig. 3. Solution u_h of one half of the reference problem.

wherein the length of the periode

$$d = d_1 + d_2 \tag{4}$$

of the lamination is included.

III. Electrostatic Problem

In this section homogenization with a multi-scale ansatz is presented in deatail. To this end the electrostatic problem shown in Figure 2 is considered.

A. Boundary value problem

The equation (5) holds in the entire problem region Ω. According to Figure 2 either Dirichlet (6) or Neumann (7) boundary conditions are prescribed on the boundary Γ. Thus, we end up with:

$$-\nabla(\lambda(x,y)\nabla u(x,y)) = 0 \qquad \text{in } \Omega \tag{5}$$

$$u = u_D \qquad \text{on } \Gamma_D \tag{6}$$

$$\lambda\frac{\partial u}{\partial n} = 0 \qquad \text{on } \Gamma_N \tag{7}$$

In case of an electrostatic problem, the material parameter λ represents the electric permittivity ϵ, and the solution variable u stands for the electric scalar potential V.

B. Weak form

Multiplication of (5) by a test function v and integration over Ω yields

$$-\int_\Omega \nabla(\lambda\nabla(u))v\,d\Omega = 0,$$

and integration by parts leads to

$$\int_\Omega \lambda\nabla u\cdot\nabla v\,d\Omega - \int_\Gamma \lambda\frac{\partial u}{\partial n}v\,d\Gamma = 0.$$

The boundary conditions (6, 7) and $v = 0$ on Γ_D leads to the weak form for the finite element method:
Find $u_h \in V_D := \{u_h \in \mathcal{V}_h : u_h = u_D \text{ on } \Gamma_D\}$, such that

$$\int_\Omega \lambda\nabla u_h\cdot\nabla v_h\,d\Omega = 0 \qquad \forall v_h \in V_0 \tag{8}$$

with $V_0 := \{v_h \in \mathcal{V}_h : v_h = 0 \text{ on } \Gamma_D\}$, where $\mathcal{V}_h$ is a finite element subspace of $H^1(\Omega)$.

C. Reference solution

Consider the specific boundary value problem represented in Figure 2. The equation (5) is solved in the subdomains Ω_m and Ω_0. Homogeneous Neumann boundary conditions are given at the top and at the bottom and inhomogeneous Dirichlet boundary conditions are prescribed on the left and right hand side. The x axis is assumed to be perpendicular to the laminations as indicated, and the origin of the coordinate system coincides with the center of the problem. First we analyze the reference solution of the electrostatic problem. The reference solution is obtained by a finite element model considering the laminations individually. The fill factor f was assumed to be 0.9, the material parameters λ_0, λ_1 and λ_2 were selected with 1, 1000 and 1, respectively. The number of laminations n was 10 in the model.

Figure 3 shows the solution u_h of one half of the problem represented in the 3^{rd} dimension, i.e. z-direction. The solution in Ω_m where the laminated medium is located exhibits a characteristic staggered or zickzack behavior as expected. The solution along the x-axis at $y = 0$, see Figure 4, can be observed as a superposition of a mean value u_0 (dashed line) with an oscillating part with $2u_1$ as the envelope (dot-dash line).

D. Micro-shape function ϕ

Additionally, we consider the periodic micro-shape function ϕ shown in Figure 5. It is adequate for the weak form in (8). The behavior of the function ϕ in x-direction is sketched in Figure 5, and it is constant in the y-direction. The dimensions of the lamination d_1 and d_2 are represented.

E. Multi-scale ansatz

Based on the observations in the above subsection C and considerations in D, respectively, the ansatz is made:

$$u(x,y) = u_0(x,y) + \phi(x)u_1(x,y) \tag{9}$$

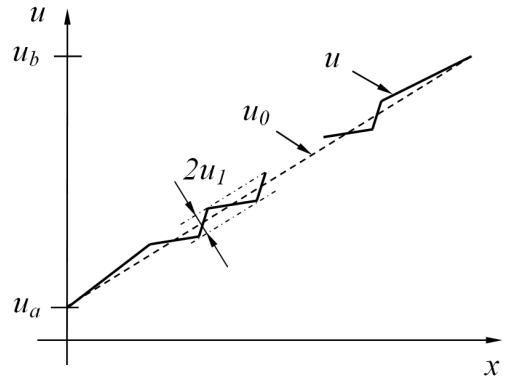

Fig. 4. Solution u along x at $y = 0$, mean value u_0 and envelope u_1.

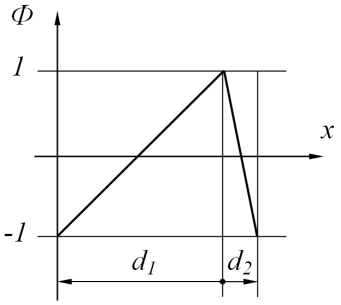

Fig. 5. Periodic micro-shape function $\phi(x)$, one periode is shown.

F. Homogenized weak form

Inserting (9) into the bilinear form of (8) yields

$$\int_\Omega \lambda(\nabla u_0 + u_1\nabla\phi + \phi\nabla u_1)\cdot(\nabla v_0 + v_1\nabla\phi + \phi\nabla v_1)\,d\Omega \quad (10)$$

and carrying out simple manipulation leads to the modified bilinear form

$$\int_\Omega \begin{pmatrix} \partial_x u_0 \\ \partial_y u_0 \\ u_1 \\ \partial_x u_1 \\ \partial_y u_1 \end{pmatrix}^T \begin{pmatrix} \lambda & 0 & \lambda\phi_x & \lambda\phi & 0 \\ 0 & \lambda & 0 & 0 & \lambda\phi \\ \lambda\phi_x & 0 & \lambda\phi_x^2 & \lambda\phi\phi_x & 0 \\ \lambda\phi & 0 & \lambda\phi\phi_x & \lambda\phi^2 & 0 \\ 0 & \lambda\phi & 0 & 0 & \lambda\phi^2 \end{pmatrix} \begin{pmatrix} \partial_x v_0 \\ \partial_y v_0 \\ v_1 \\ \partial_x v_1 \\ \partial_y v_1 \end{pmatrix} \quad (11)$$

with $\phi_x = \frac{\partial\phi}{\partial x}$. Note that $\frac{\partial\phi}{\partial y} = 0$.
The transposed vector contains the solution u, whereas the right vector the test functions v. The matrix in between represents the coefficient matrix. Coefficients are λ, $\phi\lambda$, $\nabla\phi\lambda$, $\phi^2\lambda$, etc. The function ϕ is a highly oscillating function compared to the dimensons of the laminated medium. Hence, the coefficients oscillate too.

Homogenization takes place by averaging the coefficients over the period with the length d. Thus, the oscillations are filtered out. The averaged coefficients are:

$$\begin{aligned}
\overline{\lambda} &= \frac{1}{d}\int_0^d \lambda(x)dx = \frac{\lambda_1 d_1 + \lambda_2 d_2}{d} \\
\overline{\lambda\phi_x} &= \frac{1}{d}\int_0^d \lambda(x)\phi_x(x)dx = 2\frac{\lambda_1 - \lambda_2}{d} \\
\overline{\lambda\phi} &= \frac{1}{d}\int_0^d \lambda(x)\phi(x)dx = 0 \\
\overline{\lambda\phi_x^2} &= \frac{1}{d}\int_0^d \lambda(x)\phi_x^2(x)dx = \frac{4}{d}(\frac{\lambda_1}{d_1} + \frac{\lambda_2}{d_2}) \\
\overline{\lambda\phi_x\phi} &= \frac{1}{d}\int_0^d \lambda(x)\phi_x(x)\phi(x)dx = 0 \\
\overline{\lambda\phi^2} &= \frac{1}{d}\int_0^d \lambda(x)\phi^2(x)dx = \frac{\lambda_1 d_1 + \lambda_2 d_2}{3d}
\end{aligned} \quad (12)$$

Averaged coefficients are indicated by the bar above. Some of them cancel out. Using the coefficients in (12) the homogenized bilinear form

$$\int_\Omega \begin{pmatrix} \partial_x\overline{u}_0 \\ \partial_y\overline{u}_0 \\ \overline{u}_1 \\ \partial_x\overline{u}_1 \\ \partial_y\overline{u}_1 \end{pmatrix}^T \begin{pmatrix} \overline{\lambda} & 0 & \overline{\lambda\phi_x} & 0 & 0 \\ 0 & \overline{\lambda} & 0 & 0 & 0 \\ \overline{\lambda\phi_x} & 0 & \overline{\lambda\phi_x^2} & 0 & 0 \\ 0 & 0 & 0 & \overline{\lambda\phi^2} & 0 \\ 0 & 0 & 0 & 0 & \overline{\lambda\phi^2} \end{pmatrix} \begin{pmatrix} \partial_x\overline{v}_0 \\ \partial_y\overline{v}_0 \\ \overline{v}_1 \\ \partial_x\overline{v}_1 \\ \partial_y\overline{v}_1 \end{pmatrix} \quad (13)$$

is obtained.

Numerical experiments have shown that neglecting the terms $\phi\nabla u_1$ and $\phi\nabla v_1$ in (10) yields a more accurate solution. A rigorous analysis by mixed finite elements will be presented later. Hence, the bilinear form in (13) reduces and leads to the homogenized weak form for the finite element method:
Find $(\overline{u}_{h0}, \overline{u}_{h1}) \in V_D := \{(\overline{u}_{h0}, \overline{u}_{h1}) : \overline{u}_{h0} \in \mathcal{V}_h\ ,\ \overline{u}_{h1} \in \mathcal{W}_h\ ,\ \overline{u}_{h0} = u_D \text{ on } \Gamma_D\}$, such that

$$\int_\Omega \begin{pmatrix} \partial_x\overline{u}_0 \\ \partial_y\overline{u}_0 \\ \overline{u}_1 \end{pmatrix}^T \begin{pmatrix} \overline{\lambda} & 0 & \overline{\lambda\phi_x} \\ 0 & \overline{\lambda} & 0 \\ \overline{\lambda\phi_x} & 0 & \overline{\lambda\phi_x^2} \end{pmatrix} \begin{pmatrix} \partial_x\overline{v}_0 \\ \partial_y\overline{v}_0 \\ \overline{v}_1 \end{pmatrix} d\Omega = 0 \quad (14)$$

for all $(\overline{v}_{h0}, \overline{v}_{h1}) \in V_0 := \{(\overline{v}_{h0}, \overline{v}_{h1}) : \overline{v}_{h0} \in \mathcal{V}_h\ ,\ \overline{v}_{h1} \in \mathcal{W}_h\ ,\ \overline{v}_{h0} = 0 \text{ on } \Gamma_D\}$, where $\mathcal{V}_h$ is a finite element subspace of $H^1(\Omega)$ and $\mathcal{W}_h$ a finite element subspace of $L_2(\Omega_m)$, respectively. The micro-shape function ϕ is in the space of periodic and continuous functions $H_{per}(\Omega_m)$.

The homogenized functions $\overline{u}_{h0}$ and $\overline{u}_{h1}$ are smooth functions. Thus, the homogenized medium can be modeled like a bulk by a coarse finite element mesh. There is no need for a dense mesh. Figure 6 shows the homogenized solution

$$\overline{u}_h = \overline{u}_{h0} + \phi\overline{u}_{h1}.$$

There is an excellent agreement between this solution and the reference one in Figure 2. The same can be stated comparing the fluxes

$$\Psi(x, y) = -\lambda\nabla u.$$

in Figures 7 and 8. An accurate calculation of Ψ is more demanding, because it requires the gradient of the solution. Evaluating the energy

$$W = \int_{\Omega_m} \lambda\nabla u\nabla u\,d\Omega$$

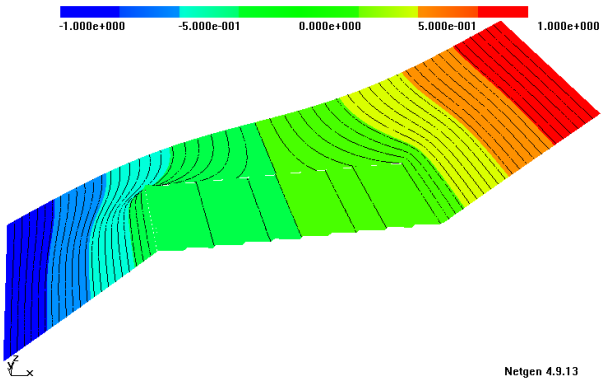

Fig. 6. Solution $\overline{u}_h$ of one half of the homogenized problem.

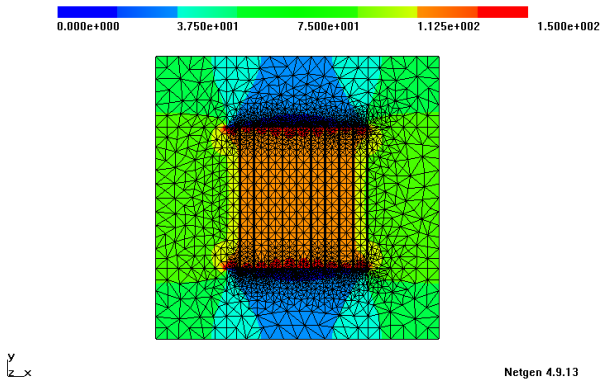

Fig. 7. Flux density of the reference problem: x-component.

of the laminated medium yields 0.586 for the reference problem and 0.608 for the homogenized problem.

IV. Eddy Current Problem

Subsequently, the eddy current problem in 2D is treated.

A. Boundary value problem

The boundary value problem is shown in Figure 9. It consists of laminated iron Ω_m enclosed by air Ω_0. On the boundary $\Gamma = \Gamma_H \cup \Gamma_B$ either the tangential component

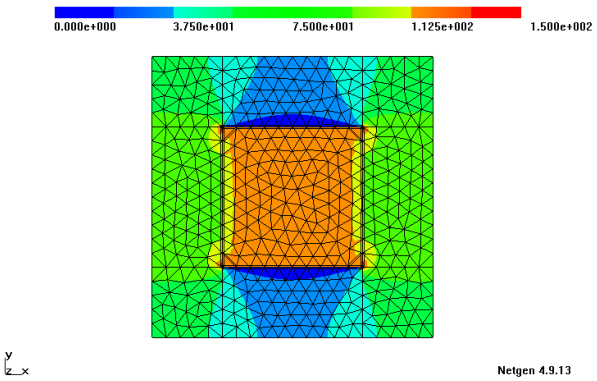

Fig. 8. Flux density of the homogenized problem: x-component.

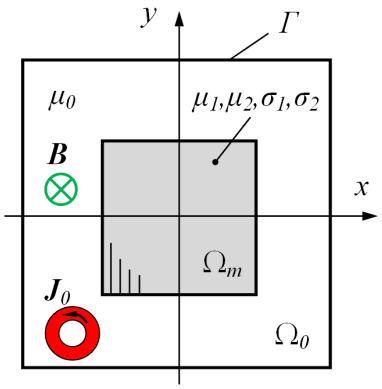

Fig. 9. Eddy current boundary value problem.

of the magnetic field intensity $(\boldsymbol{H})_t$ on Γ_H or the normal component of the magnetic flux density $(\boldsymbol{B})_n$ on Γ_B is prescribed. The eddy current problem, where the magnetic flux density $\boldsymbol{B}$ is perpendicular to the plane of projection, is studied in this paper. The electric conductivity σ and the magnetic permeability μ are assumed to be linear. The time harmonic case in the steady state is considered. Due to this assumptions the Maxwell's equations are represented in the complex representation, where j stands for the imaginary unit and ω for the angular frequency:

$$\operatorname{curl}\boldsymbol{H} = \boldsymbol{J} \quad \text{in } \Omega_m \tag{15}$$
$$\operatorname{curl}\boldsymbol{E} = -j\omega\boldsymbol{B} \tag{16}$$
$$\operatorname{div}\boldsymbol{B} = 0 \tag{17}$$
$$\boldsymbol{J} = \sigma\boldsymbol{E} \tag{18}$$
$$\boldsymbol{B} = \mu\boldsymbol{H} \tag{19}$$

$$\operatorname{curl}\boldsymbol{H} = \boldsymbol{J}_0 \quad \text{in } \Omega_0 \tag{20}$$
$$\operatorname{div}\boldsymbol{B} = 0 \tag{21}$$
$$\boldsymbol{B} = \mu\boldsymbol{H} \tag{22}$$

$$\boldsymbol{H}\times\boldsymbol{n} = \boldsymbol{K} \quad \text{on } \Gamma_H \tag{23}$$
$$\boldsymbol{B}\cdot\boldsymbol{n} = b \quad \text{on } \Gamma_B \tag{24}$$

Relations (15) to (19) are valid in Ω_m, whereas (20) to (22) belong to air Ω_0 and (23, 24) are boundary conditions. Due to (17) and (21) the magnetic vector potential $\boldsymbol{A}$ can be introduced as

$$\boldsymbol{B} = \operatorname{curl}\boldsymbol{A}.$$

With the aid of Faraday's law (16), the electric field intensity $\boldsymbol{E}$ can be written as

$$\boldsymbol{E} = -j\omega\boldsymbol{A}.$$

Ampere's law (15) leads to the partial differential equation

$$\operatorname{curl}\mu^{-1}\operatorname{curl}\mathbf{A} + j\omega\sigma\mathbf{A} = \boldsymbol{J}_0 \text{ in } \Omega \tag{25}$$

with the impressed current density $\boldsymbol{J}_0$. Introducing $\boldsymbol{A}$ in (23) and (24) yields the boundary conditions

$$\mu^{-1}\operatorname{curl}\boldsymbol{A}\times\boldsymbol{n} = \boldsymbol{K} \quad \text{on } \Gamma_H \tag{26}$$
$$\boldsymbol{A}\times\boldsymbol{n} = \alpha \quad \text{on } \Gamma_B, \tag{27}$$

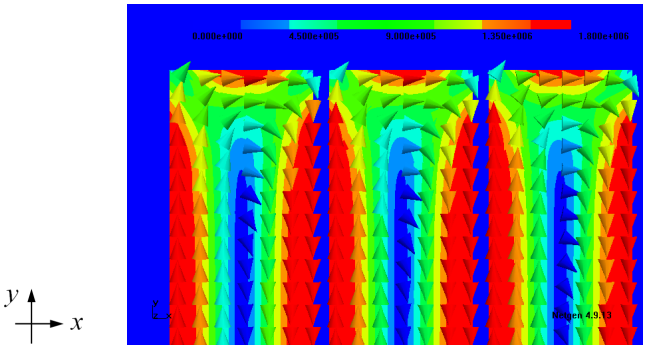

Fig. 10. Detail of the eddy current distribution in laminations in the upper left corner, reference solution.

where $\boldsymbol{K}$ is the surface current density and α means the magnetic flux.

B. Weak form

Multiplication of (25) by a test function $\boldsymbol{\nu}$ and integration over Ω yields

$$\int_\Omega (\operatorname{curl}\mu^{-1}\ \operatorname{curl}\boldsymbol{A})\boldsymbol{\nu}\ d\Omega + j\omega\int_{\Omega_m}\sigma\boldsymbol{A}\boldsymbol{\nu}\ d\Omega = \int_{\Omega_0}\boldsymbol{J}_0\boldsymbol{\nu}\ d\Omega.$$

Integration by parts leads to

$$\int_\Omega \mu^{-1}\ \operatorname{curl}\boldsymbol{A}\ \operatorname{curl}\boldsymbol{\nu}\ d\Omega + \int_\Gamma \mu^{-1}\ \operatorname{curl}\boldsymbol{A}\times\boldsymbol{\nu}\boldsymbol{n}\ d\Gamma + j\omega\int_{\Omega_m}\sigma\boldsymbol{A}\boldsymbol{\nu}\ d\Omega = \int_{\Omega_0}\boldsymbol{J}_0\boldsymbol{\nu}\ d\Omega.$$

Homogeneous boundary conditions on Γ_H and $\boldsymbol{\nu}\times\boldsymbol{n} = \boldsymbol{0}$ on Γ_B lead to the weak form for the finite element method:
Find $\boldsymbol{A}_h \in V_B := \{\boldsymbol{A}_h \in \mathcal{V}_h : \boldsymbol{A}_h\times\boldsymbol{n} = \alpha_h \text{ on } \Gamma_B\}$, such that

$$\int_\Omega \mu^{-1}\operatorname{curl}\boldsymbol{A}_h\operatorname{curl}\boldsymbol{\nu}_h\,d\Omega + j\omega\int_\Omega\sigma\boldsymbol{A}_h\boldsymbol{\nu}_h\,d\Omega = \int_{\Omega_0}\boldsymbol{J}_0\boldsymbol{\nu}_h\,d\Omega \tag{28}$$

for all $\boldsymbol{\nu}_h \in V_0 := \{\boldsymbol{\nu}_h \in \mathcal{V}_h : \boldsymbol{\nu}_h\times\boldsymbol{n} = \boldsymbol{0} \text{ on } \Gamma_B\}$, where $\mathcal{V}_h$ is a finite element subspace of $H(\operatorname{curl},\Omega)$.

C. Multi-scale ansatz

To derive a suitable ansatz for $\boldsymbol{A}$, the eddy current distribution in laminations in a reference problem as shown in Figure 10 is studied (see also Figure 11). Eddy currents are confined to flow in narrow loops. They exhibit essentially a y-component $(\boldsymbol{J})_y$, except at the edges of the laminations, where the eddy currents turn around and the x-component $(\boldsymbol{J})_x$ dominates. Based on these observations the approach

$$\boldsymbol{A} = \boldsymbol{A}_0 + \phi\begin{pmatrix}0\\A_1\end{pmatrix} + \nabla(\phi w) \tag{29}$$

has been derived. In (29) $\boldsymbol{A}_0$ means the mean value, ϕ times the vector with the only entry A_1 at the y-component models $(\boldsymbol{J})_y$, and the last term take account of $(\boldsymbol{J})_x$. A_1 and w are scalar functions. The micro-shape function ϕ is the same as in section III. D.

D. Homogenized weak form

Introducing (29) in the bilinear form of (28) leads to the modified bilinear form

$$\begin{aligned}\int_\Omega \mu^{-1}\Big[&\operatorname{curl}\left(\boldsymbol{A}_0 + \phi(0,A_1)^T + \nabla(\phi w)\right)\\ &\cdot\operatorname{curl}\left(\boldsymbol{\nu}_0 + \phi(0,v_1)^T + \nabla(\phi q)\right)\Big]\,d\Omega\\ + j\omega\int_\Omega\sigma\Big[&\left(\boldsymbol{A}_0 + \phi(0,A_1)^T + \nabla(\phi w)\right)\\ &\cdot\left(\boldsymbol{\nu}_0 + \phi(0,v_1)^T + \nabla(\phi q)\right)\Big]\,d\Omega\\ = \int_{\Omega_0}&\boldsymbol{J}_0\boldsymbol{\nu}_0\,d\Omega,\end{aligned} \tag{30}$$

where the test functions v_1 and q vanish in Ω_0.

Simple manipulations, neglecting the derivative of A_1 (for the same reasons as in III. F) and carrying out homogenization the first bilinear form in (30) reads as

$$A(\overline{\boldsymbol{A}}_0,\overline{A}_1;\overline{\boldsymbol{\nu}}_0,\overline{v}_1) = \int_\Omega\begin{pmatrix}\operatorname{curl}\overline{\boldsymbol{A}}_0\\ \overline{A}_1\end{pmatrix}^T\overline{S}_1\begin{pmatrix}\operatorname{curl}\overline{\boldsymbol{\nu}}_0\\ \overline{v}_1\end{pmatrix}d\Omega, \tag{31}$$

where

$$\overline{S}_1 = \begin{pmatrix}\overline{\nu} & \overline{\nu\phi_x}\\ \overline{\nu\phi_x} & \overline{\nu\phi_x^2}\end{pmatrix}$$

with the magnetic reluctivity $\nu = \mu^{-1}$. The coefficients in $\overline{S}_1$ were averaged, see (12). Homogenization of the second bilinear form in (30) yields

$$B(\overline{\boldsymbol{A}}_0,\overline{A}_1,\overline{w};\overline{\boldsymbol{\nu}}_0,\overline{v}_1,\overline{q}) = j\omega\int_\Omega\begin{pmatrix}(\overline{\boldsymbol{A}}_0)_x\\(\overline{\boldsymbol{A}}_0)_y\\\overline{A}_1\\\overline{w}\\\partial_x\overline{w}\\\partial_y\overline{w}\end{pmatrix}^T\overline{M}_1\begin{pmatrix}(\overline{\boldsymbol{\nu}}_0)_x\\(\overline{\boldsymbol{\nu}}_0)_y\\\overline{v}_1\\\overline{q}\\\partial_x\overline{q}\\\partial_y\overline{q}\end{pmatrix}d\Omega \tag{32}$$

with

$$\overline{M}_1 = \begin{pmatrix}\overline{\sigma} & 0 & 0 & \overline{\sigma\phi_x} & 0 & 0\\ 0 & \overline{\sigma} & 0 & 0 & 0 & 0\\ 0 & 0 & \overline{\sigma\phi^2} & 0 & 0 & \overline{\sigma\phi^2}\\ \overline{\sigma\phi_x} & 0 & 0 & \overline{\sigma\phi_x^2} & 0 & 0\\ 0 & 0 & 0 & 0 & \overline{\sigma\phi^2} & 0\\ 0 & 0 & \overline{\sigma\phi^2} & 0 & 0 & \overline{\sigma\phi^2}\end{pmatrix}. \tag{33}$$

The coefficients in (33) were averaged, see (12). The linear form in (30) is denoted by $f(\boldsymbol{\nu}_0)$. Considering (31) to (34) the homogenized weak form for the finite element method reads as follows:
Find $(\overline{\boldsymbol{A}}_{0h},\overline{A}_{1h},\overline{w}_h) \in V_B := \{(\overline{\boldsymbol{A}}_{0h}\ ,\ \overline{A}_{1h}\ ,\ \overline{w}_h) : \overline{\boldsymbol{A}}_{0h} \in \mathcal{U}_h\ ,\ \overline{A}_{1h}\in\mathcal{V}_h\ ,\ \overline{w}_h\in\mathcal{W}_h \text{ and } \overline{\boldsymbol{A}}_{0h}\times\boldsymbol{n} = \alpha_h \text{ on } \Gamma_B\}$, such that

$$A(\overline{\boldsymbol{A}}_{0h},\overline{A}_{1h};\overline{\boldsymbol{\nu}}_{0h},\overline{v}_{1h}) + B(\overline{\boldsymbol{A}}_{0h},\overline{A}_{1h},\overline{w}_h;\overline{\boldsymbol{\nu}}_{0h},\overline{v}_{1h},\overline{q}_h) = f(\boldsymbol{\nu}_{0h}) \tag{34}$$

for all $(\overline{\boldsymbol{\nu}}_{0h},\overline{v}_{1h},\overline{q}_h) \in V_0 := \{(\overline{\boldsymbol{\nu}}_{0h}\ ,\ \overline{v}_{1h}\ ,\ \overline{q}_h) : \overline{\boldsymbol{\nu}}_{0h}\in\mathcal{U}_h, \overline{v}_{1h}\in\mathcal{V}_h\ ,\ \overline{q}_h\in\mathcal{W}_h \text{ and } \overline{\boldsymbol{\nu}}_{0h}\times\boldsymbol{n} = \boldsymbol{0} \text{ on } \Gamma_B\}$, where $\mathcal{U}_h$ is a finite element subspace of $H(\operatorname{curl},\Omega)$, $\mathcal{V}_h$ a finite element subspace of $L_2(\Omega_m)$ and $\mathcal{W}_h$ a finite element subspace of $H^1(\Omega_m)$, respectively. The micro-shape function ϕ is in the space of periodic and continuous functions $H_{per}(\Omega_m)$.

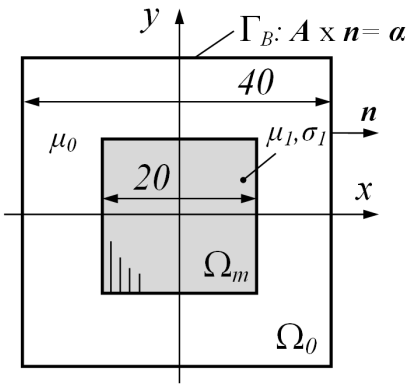

Fig. 11. Numerical example of an eddy current problem, dimensions in mm.

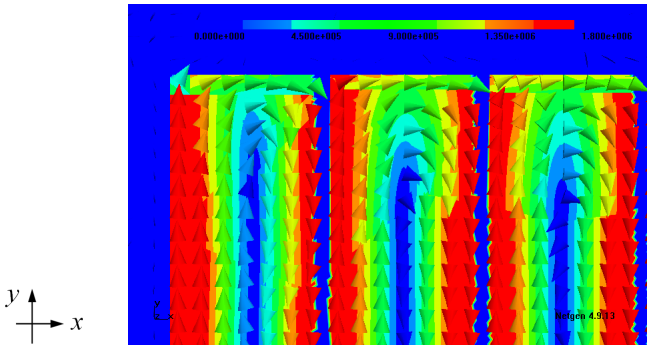

Fig. 12. Detail of the eddy current distribution in laminations in the upper left corner, homogenized solution.

The alternative multi-scale ansatz to (29)

$$\boldsymbol{A} = \boldsymbol{A}_0 + \phi \begin{pmatrix} 0 \\ A_1 \end{pmatrix} + \phi \nabla w \tag{35}$$

has been derived, too. Analog steps as in (30) to (34) have been carried out for (35) to obtain the associated homogenized weak form.

V. Numerical Example

The numerical example is shown in Figure 11. Boundary conditions are prescribed for the tangential component of $(\mathbf{A_0})_\mathbf{t}$ on Γ such that a total magnetic flux of $1.6mVs/m^2$ flows perpendicularly through the domain Ω. A rather unfavorable fill factor of $f = 0.9$, a relative permeability of $\mu_r = 1000$, a conductivity of $\sigma = 2 \cdot 10^6 S/m$ and a frequency of $50Hz$ were selected. This leads to a penetration depth of

$$\delta = \sqrt{\frac{2}{2\pi f \mu \sigma}} = 1.6mm$$

in iron. The gap between the laminations and Ω_0 were assumed to be air.

Comparing the eddy current distribution obtained by the homogenized method represented in Figure 12 with that obtained by the reference model in Figure 11, a fairly good agreement can be observed. The thickness of the laminations d_1 was equal to $1.8mm$.

An accurate calculation of the eddy current losses is of particular interest in the context of eddy currents in laminated iron. To this end a study of these losses for different thicknesses of laminations has been carried out. The losses are summarized in Table I. In general, there is a very satisfactory agreement between the losses obtained by the alternative multi-scale approaches and those of the reference solution. The error increases with the thickness d as expect. The method with the ansatz in (29) delivers losses with appreciable smaller errors than that with (35).

TABLE I
Comparison of Calculated Eddy Current Losses

Losses in W/m			
d in mm	Reference	Ansatz $\nabla(\phi w)$	Ansatz $\phi\nabla(w)$
0.5	11.59	11.58	11.48
1.0	45.70	45.46	44.74
2.0	177.2	174.16	169.4

To figure out the computational costs the number of the finite elements NFE and the number of degrees of freedom NDOF are given in Table II for the reference model and for the homogenized ones for the case where d equals to $0.5mm$. The number of laminations was 40. It can easily be seen that the computational costs what the memory requirement concerns of the homogenized models are essentially smaller than those of the reference model.

TABLE II
Computational Costs

Model	FE	NDOF
Reference	104 452	783 555
Homogenized	1 286	11 117

FE No. finite elements
NDOF No. degrees of freedom

References

[1] S. Nogawa, M. Kuwata, T. Nakau, D. Miyagi, and N. Takahashi, "Study of Modeling Method of Lamination of Reactor Core," IEEE Trans. Magn., vol. 42, no. 4, pp. 1455-1458, April 2006.

[2] V. C. Silva, G. Meunier, and A. Foggia, "A 3D finite element computation of eddy currents and losses in laminated iron cores allowing for the electric and magnetic anisotropy," IEEE Trans. Magn., vol. 31, pp. 2139-2141, May 1995.

[3] H. Kaimori, A. Kameari, and K. Fujiwara, "FEM Computation of Magnetic Field and Iron Loss in Laminated Iron Core Using Homogenization Method," IEEE Trans. Magn., vol. 43, no. 4, pp. 1405-1408, April 2007.

[4] K. Hollaus, and O. Bíró, "Estimation of 3D eddy currents in conducting laminations by an anisotropic conductivity and a 1Danalytical solution," COMPEL, vol. 18, no. 3, pp. 494-503, 1999.

[5] K. Hollaus, and O. Bíró, "A FEM formulation to treat 3D eddy current in laminations," IEEE Trans. Magn., vol. 36, no. 5, pp. 1289-1292, Sep. 2000.

[6] I. Sebestyén, S. Gyimóthy, J. Pávó, and O. Bíró, "Calculation of Losses in Laminated Ferromagnetic Materials," IEEE Trans. Magn., vol. 40, no. 2, pp. 924-927, March 2004.

[7] O. Bíró, K. Preis, and I. Ticar, "A FEM method for eddy current analysis in laminated media," COMPEL, vol. 24, no. 1, pp. 241-248, 2005.

[8] P. Dular et al., "A 3-D magnetic vector potential formulation taking eddy currents in lamination stacks into account," IEEE Trans. Magn., vol. 39, pp. 1147-1150, May 2003.

[9] L. Krähenbühl, P. Dular, T. Zeidan, and F. Buret, "Homogenization of Lamination Stacks in Linear Magnetodynamics," IEEE Trans. Magn., vol. 40, no. 2, pp. 912-915, March 2004.